II.H.7 Theory of Oxides for Photo-Electrochemical Hydrogen Production

Yanfa Yan (Primary Contact),
Muhammad Huda, Aron Walsh, Su-Huai Wei,
Mowafak Al-Jassim, and John Turner

National Renewable Energy Laboratory (NREL)
1617 Cole Blvd.
Golden, CO 80401
Phone: (303) 384-6456; Fax: (303) 384-6604
E-mail: yanfa.yan@nrel.gov

DOE Technology Development Manager:
Roxanne Garland

Phone: (202) 586-7260; Fax: (202) 586-2373
E-mail: Roxanne.Garland@ee.doe.gov

Project Start Date: 2007
Project End Date: Project continuation and
direction determined annually by DOE

Objectives

The main focus of the project is to:

- Understand the performance of current photoelectrochemical (PEC) materials.
- Provide guidance and solution for performance improvement.
- Design and discover new materials.
- Provide theoretical basis for Go/No-Go decisions to DOE PEC H_2 projects.

Technical Barriers

This project addresses the following technical barriers from the PEC Water Splitting section of the Hydrogen, Fuel Cells and Infrastructure Technologies Program Multi-Year Research, Development and Demonstration Plan:

(C) Photon Absorption Coefficient

(F) Optical and Transport Properties

(X) Stability in Aqueous Solutions

Technical Targets

This project is intended to provide theoretical understanding of the performance of current PEC materials and provide feedback and guidance for performance improvement.

Accomplishments

- Understood the electronic properties of Fe_2O_3 and the key limiting factors for Fe_2O_3 as electrodes in PEC water splitting.
- Understood the effects of doping with transition metal on the PEC performance of Fe_2O_3.
- Understood the electronic properties of $BiVO_4$ and explained why $BiVO_4$ could be a good candidate for PEC water splitting.

✧   ✧   ✧   ✧   ✧

Introduction

A large number of metal oxides have been under investigation for potential use as electrodes for solar PEC water splitting for hydrogen production. This project is aimed to provide theoretical understanding of the performance of current PEC materials and provide feedback and guidance for performance improvement. In this report, two materials, the Fe_2O_3 hematite, and $BiVO_4$ are studied theoretically. The problems associated with these materials are identified and corresponding suggestions for overcoming the problems are provided.

Hematite (α-Fe_2O_3) has long been of interest as a potential PEC material because it is among the most abundant and inexpensive semiconductors on earth with a bandgap (~2.1 eV) that is appropriate for water splitting. Hematite is stable in most electrolytes at $pH > 3$ and it is non-toxic. Unfortunately, pure-phase hematite is a charge transfer-type Mott insulator with intrinsically poor conductivity (by small polarons) which limits the quantum efficiency for any PEC process. To improve upon hematite's intrinsic electronic properties, substitutional doping with Si, Ti, Pt, Mo, Cr, and Ge, among other atoms, has been reported [1-5]. It is critical to understand why and how these substitutional doping could improve the hematite's electronic properties. $BiVO_4$ has shown particular promise for water photodecomposition with the presence of both a low band gap (2.4 – 2.5 eV) and reasonable band edge alignment with respect to the water redox potentials [6]. It has been reported to exhibit both n and p-type semiconducting properties [7], in addition to high photon-to-current conversion efficiencies. However, to date, the fundamental electronic structure of $BiVO_4$ has not been well explored. In particular, it is unclear whether the band gap is direct or indirect, and what role the occupied Bi 6s lone pair electrons may play in determining the valence band edge positions and charge transport. It is necessary to thoroughly understand the electronic structure of $BiVO_4$.

Approach

Calculations were performed using density functional theory (DFT) as implemented in the Vienna ab initio simulation package (VASP) code [8]. Three dimensional periodic boundary conditions were used to approximate an infinite solid. Gradient corrected exchange-correlation effects were described within the Perdew-Burke-Ernzerhof (PBE) functional. The core electrons were treated within the projector augmented wave (PAW) method. Both the optical transition matrix elements and optical absorption spectrum were calculated within the transversal approximation and the PAW method for $BiVO_4$. For α-Fe_2O_3, as Fe-d band is partially filled highly localized band, a $U = 5.5$ eV has been added to the DFT Hamiltonian. We have tested that without any U the magnetic ordering of α-Fe_2O_3 was not correct, and the band gap was highly underestimated. With U the band gap was found to be 1.72 eV, whereas the experimental band gap is 2.2 eV. The primitive unit cell of α-Fe_2O_3 is in rhombohedral symmetry. However, this unit cell cannot accommodate the anti-ferromagnetic (AFM) ordering as manifested by α-Fe_2O_3. So a more conventional unit cell with 12 Fe atoms and 18 O atoms were taken as a supercell. This supercell, shown in Figure 1(a), has a layer by layer structure where each layer of Fe atoms is separated by O atoms. In addition, each layer of Fe atoms has parallel (either up or down) spin configurations, and the overall magnetic configuration is manifested here as layer-by-layer AFM. This particular magnetic configuration plays an important part in the conduction properties of this material.

Results

We first discuss why pure α-Fe_2O_3 does not have good conductivity. Figure 1 (a) shows an Fe_2O_3 super cell, while Figure 1 (b) shows the calculated band structure for α-Fe_2O_3. The main feature of the band structure is that the conduction band minima (CBM) between the M and K points in the brillouin zone is almost completely flat, indicating extremely high electron effective mass. The lower part of the conduction band between Γ and A is also very flat. It implies that inter-layer conduction along z-direction is also highly suppressed, and is known to be four times lower than that along the layer conduction. So, electron conduction in α-Fe_2O_3 basically takes place along the same layers where all the Fe atoms have unidirectional magnetic moment. In other words, n-type α-Fe_2O_3 would not have good electron conductivity. Thus, despite the favorable band gap of around 2 eV, pure α-Fe_2O_3 does not exhibit good PEC photo-response. On the other hand, valence band maxima lies between M and K points, has some dispersion feature. This gives holes a little less effective mass than the electrons. Site projected density of states clearly shows that the presence of highly localized Fe $3d$ band is responsible for the high electron effective mass. Because of this factor, the electron conductivity in α-Fe_2O_3 is realized through small polaron hopping. The band structure further indicates that electron hopping between the Fe-atoms in the same layers is more probable than between the inter-layer Fe atoms.

To improve the PEC performance, α-Fe_2O_3 has been doped with various transition metals, such as Ti, V, Cr, Ni, Pt, … While some dopants, such as Ti, Pt, and Cr showed significant improvement in the performance, some dopants, such as Mn, showed the opposite effects. The calculated band structures for Ti doped α-Fe_2O_3 are shown in Figure 2. Although Ti can also have 3+ oxidation states (such as in Ti_2O_3), here the substitution is not isovalent. From the spin down band structure, it is seen that the CBM is heavily modified because of the presence of Ti. The CBM are more dispersive than that of the pristine α-Fe_2O_3. Thus, the electron

FIGURE 1. (a) Fe_2O_3 super cell with AFM arrangements. Red and golden balls are oxygen and iron atoms, respectively. (b) Calculated band structure of Fe_2O_3.
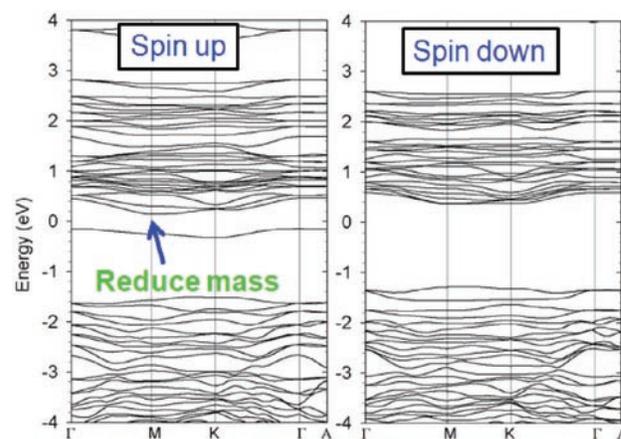
FIGURE 2. Calculated Band Structure (a) Spin Up, (b) Spin Down for Ti doped Fe_2O_3

effective mass of α-Fe_2O_3 is reduced significantly after doping with Ti. The band structures further reveal that the Ti levels below CBM is partially filled indicating that Ti doped α-Fe_2O_3 would behave as an *n*-type material. These results suggest that Ti doping in α-Fe_2O_3 would significantly improve the conductivity and therefore enhance the PEC performance as observed experimentally.

We have calculated the band structures for α-Fe_2O_3 doped with other transition metals. We found that Pt and Cr also modify the CBM of α-Fe_2O_3, leading to more dispersive CBM and therefore reduced electron effective mass and improved electron conductivity. These explain why Pt and Cr doping would enhance the photo-response for α-Fe_2O_3. However, doping with Mn does not change the dispersion of CBM of α-Fe_2O_3, meaning no improvement on the electronic conductivity. In fact, Mn would create more localized defect bands leading to possible increased carrier recombination, explaining why Mn doped α-Fe_2O_3 showed even decreased performance.

We have further proposed that Ti and N codoping may lead to even improved PEC performance. This is because Ti and N codoping leads to the following effects.: 1) enhancing the doping solubility for both Ti and N; 2) increasing optical absorption in the energy region near the band gap of α-Fe_2O_3 (2.2 eV); and 3) improving electron conductivity. Our results therefore provide suggestion for further performance improvement for α-Fe_2O_3.

$BiVO_4$ (Figure 3) is a promising photocatalyst for hydrogen generation, with demonstrated experimental potential in terms of band gap, stability and conductivity. We have performed a first-principles electronic structure investigation to understand why this material is a good photocatalyst, in order to design new and better materials.

The band structure, drawn along two high symmetry lines of the Brillouin zone is shown in Figure 4. $BiVO_4$ is found to be a direct band gap insulator. While the PBE-DFT band gap of 2.16 eV is marginally underestimated relative to the experiment (2.4 – 2.5 eV), the difference is much less than metal oxides with s-like conduction bands such as ZnO (ΔE_g >2 eV). Quite unusually, both the valence and conduction band extrema are found away from the gamma point. While there is some curvature at the band edges, the high density of states around the band gap means that the bands are far from parabolic and are therefore not expected to be well described under a typical semiconductor effective mass approximation. However, fitting the energy-momentum dependence of the states along the A-M line predicts effective masses on the order of 0.3 m_e for both holes and electrons; in metal oxides typically the hole masses are much heavier, e.g. 16 m_e for In_2O_3.

To gain a deeper understanding of the band structure features, we have plotted projections of the wavefunction for three specific bands at the A point through a (001) plane containing both Bi and V atoms, labeled i, ii and iii in Figure 4. The first projection at –9.1 eV is of predominately Bi 6s character (as expected from the corresponding DOS in this energy range); significant hybridization between Bi and the neighboring

FIGURE 3. Representation of the crystal structure of $BiVO_4$. The base centered monoclinic primitive cell is indicated by the dashed black lines.
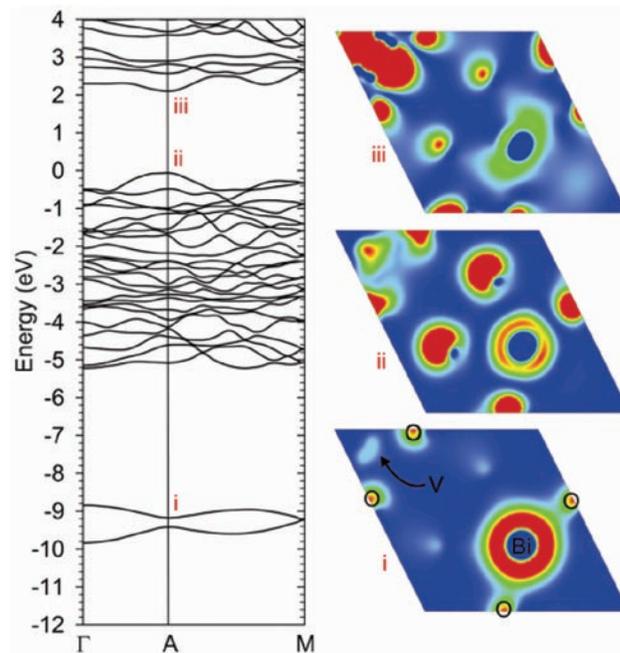
FIGURE 4. Calculated electronic band structure along the Γ-A-M lines. The highest occupied state is set to 0 eV. Charge density contour plots are shown for three bands at the A point (plotted from 0 to 0.01 e.Å^{-3}).

O can also be observed. The second projection at 0 eV is dominated by Bi and O character. Here the density node between Bi and O is suggestive of the antibonding nature of their interaction. Due to the role of symmetry and orbital phase constraints, Bi s – O p coupling does not occur at the gamma point, which results in the upwards dispersion towards A, where this interaction is maximized. The final projection is of the conduction band minimum states, which contains contributions from V d, O p and Bi p. The resulting energy level interactions are summarized in Figure 4. At gamma, the valence and conduction band extrema contain contributions solely from O 2p and V 3d, respectively. Away from the zone centre, coupling with Bi s (valence band) and Bi p/O p (conduction band) is observed. Quantitatively, the Bi s – O p interaction results in a 0.4 eV energy raise in the valence band maxima.

Conclusions and Future Directions

We have calculated the electronic structure of α-Fe$_2$O$_3$ and BiVO$_4$, using DFT. We have provided detailed understanding on why pure α-Fe$_2$O$_3$ would not exhibit very good PEC response, and why doping with some transition elements would lead to improved performance, but doping with other transition metals lead to decreased performance. We proposed a method on how to further improve the PEC performance for α-Fe$_2$O$_3$. For BiVO$_4$, we found that BiVO$_4$ is a direct band gap semiconductor, despite having band extrema away from the Brillouin zone center. Coupling between Bi 6s and O 2p forces an upward dispersion of the valence band at the zone boundary; however, a direct gap is maintained via coupling between V 3d, O 2p and Bi 6p, which lowers the conduction band minimum. These interactions result in symmetric hole and electron masses. Implications for the design of ambipolar metal oxides are discussed.

Future Directions

- Extend our research to other metal oxides.
- Design new metal oxides with desirable optical absorption, band edge positions, and transport properties.
- Extend our study to non-oxide materials, such as nitrides, carbides, sulfides, …

FY 2009 Publications/Presentations

1. M.N. Huda, Yanfa Yan, C.-Y. Moon, S.-H. Wei, and M.M. Al-Jassim, "Density-functional theory study of the effects of atomic impurity on the band edges of monoclinic WO$_3$," *Phys. Rev B* **77**, 195102 (2008).

2. Aron Walsh, Yanfa Yan, M.M. Al-Jassim, and S.-H. Wei, "Electronic, Energetic, and Chemical Effects of Intrinsic Defects and Fe-Doping of CoAl$_2$O$_4$: A DFT+*U* Study," *J. Phys. Chem. C* **112**; 12044 (2208).

3. M.N. Huda, Yanfa Yan, S.-H. Wei, and M.M. Al-Jassim, "Electronic structure of ZnO:GaN compounds: Asymmetric bandgap engineering," *Phys. Rev. B* 78, 195204 (2008).

4. Aron Walsh, Yanfa Yan, M.N. Huda, M.M. Al-Jassim, and S-H. Wei, "Band Edge Electronic Structure of BiVO4: Elucidating the Role of the Bi s and V d Orbitals," *Chem. Mater.*, *21*, 547–551(2009).

5. M.N. Huda, Yanfa Yan, S.-H. Wei, and M.M. Al-Jassim, "An Electronic Structure Study of Intermediate Band by Non-Magnetic Ion Doping in WO$_3$," 2008 MRS Fall Meeting, Boston

6. Yanfa Yan, A. Walsh, M.N. Huda, S.H. Wei, M.M. Al-Jassim, Y.S. Hu, E. McFarland, "Understanding the PEC performance of Fe$_2$O$_3$," DOE PEC H$_2$ working group meeting, Hawaii, 2008

References

1. A. Kay, I. Cesar, M. Gratzel, *J. Am. Chem. Soc.*, **128**, 15714, (2006).

2. J.H. Kennedy, M. Anderman, R. Shinar, *J. Electrochem. Soc.*, **128**, 2371, (1981).

3. J.A. Glasscock, P.R.F. Barnes, I.C. Plumb, N. Savvides, *J. Phys. Chem. C*, **111**, 16477, (2007).

4. Y.S. Hu, A. Kleiman-Shwarsctein, A.J. Forman, D. Hazen, J.N. Park, E.W. McFarland, *Chem. Mat.*, **20**, 3803, (2008).

5. A. Kleiman-Shwarsctein, Y.S. Hu, A.J. Forman, G.D. Stucky, E.W. McFarland, *J. Phys. Chem. C*, **112**, 15900, (2008).

6. Sayama, K.; Nomura, A.; Arai, T.; Sugita, T.; Abe, R.; Yanagida, M.; Oi, T.; Iwasaki, Y.; Abe, Y.; Sugihara, H. *J. Phys. Chem. B* **2006**, *110*, 11352.

7. I.C. Vinke, J. Diepgrond, B.A. Boukamp, K.J. de Vries, A.J. Burggraaf, *Solid State Ionics*, **57**, 83 (1992).

8. G. Kresse, J. Furthmüller, *Comput. Mater. Sci.*, **6**, 15 (1996).